Optical and Quantum Electronics (2019) 51:136
https://doi.org/10.1007/s11082-019-1859-z

High resolution for confocal fluorescence microscopy via extending zero-region of super-oscillation

Vannhu Le[1,2]

Received: 26 January 2019 / Accepted: 19 April 2019

Abstract
Superoscillation is the phenomenon that is observed when a wave oscillates locally faster than its highest Fourier component. Although previous reports have been shown that the superoscillation is highly attractive for imaging, however, the small zero-region area of the superoscillation increases the remarkable effect of the outsidelobes. In this work, we introduce a method using a binary phase mask with radial polarization to extend the zero-region of the superoscillation for high numerical aperture objectives. We successfully design a binary phase mask combining with a radial polarization to obtain a big zero-region of the superoscillation. Evaluation methods rely on point spread function and simulation images are presented. The results demonstrate that our proposed method is very effective for suppressing the outsidelobes. In addition, we show that our technique becomes more effective by adding an amplitude mask.

Keywords Confocal fluorescence microscopy · Polarization · Superresolution · Superoscillation

1 Introduction

The point spread function (PSF) is a powerful tool which is used to evaluate the imaging performance of optical focusing systems (Le et al. 2018; Wan et al. 2014). However, the full width at half maximum (FWHM) of the PSF, which represents the resolution of the optical system, is related to the wavelength of illuminating light and the FWHM of the PSF is limited by the diffraction limit. For visible light, the best acquired resolution is around 200 nm (Segawa et al. 2014). In the past decades, a lot of research effort has been dedicated to narrowing the PSF to achieve super-resolution and overcome the diffraction limit. Common methods are used such as stimulated emission depletion (STED) microscopy (Hell and Wichmann 1994; Gao et al. 2017), structured illumination microscopy (SIM) (Rust et al. 2006; Huang et al. 2008), stochastic optical reconstruction microscopy (STROM) (Betzig

✉ Vannhu Le
levannhu_mta2013@yahoo.com

[1] Institute of Research and Development, Duy Tan University, Da Nang 550000, Vietnam

[2] Department of Optical Engineering, Le Quy Don Technical University, 236 Hoang Quoc Viet Street, Tu Liem District, Hanoi, Vietnam

Published online: 22 April 2019

et al. 2006; Hess et al. 2006), photoactivated localization microscopy (PALM) (Classen et al. 2017; Gustafsson 2005), fluorescence emission different (FED) microscopy (Kuang et al. 2013; Korobcheyvskaya et al. 2016) and so on. While the superresolution methods are useful for many practical applications, they suffer various disadvantages, such as stringent proximity restrictions, material system limitations, and heavy needs for pre-labeling, fine-step scanning, and the post-processing of collected image data, time-consuming 3D image data processing. Therefore, the development of these technologies and the search for simpler super-resolution techniques remain important research topics.

The description of superoscillation begins with both physics and mathematics (Aharonov and Vaidman 1990; Ferreira and Kempf 2006; Aharonov et al. 1998), which have been introduced into microscopic imaging as a new way to achieve super-resolution. Superoscillation refers to the phenomenon that is observed when the oscillation of a band-limited function can be more quickly than its fastest Fourier component. Superoscillation microscopy could achieve a resolution beyond the Abbe's diffraction limit without the help of the evanescent wave. What's more, superoscillation microscopy can survive for a relatively long time before fading away due to its complex momenta (Berry and Popescu 2006), and can transfer high-frequency information farther than several wavelengths. However, there exists a major drawback to be the inevitable existence of high-energy regions away from the outsidelobes of the superoscillation, which leads to trade-off between the duration and the effective bandwidth of the superoscillation region (Ferreira and Kempf 2006). If managed unsuitably, these sidebands of superoscillation have been proven problematic when they spillover, drowning out the superoscillating signal (Berry and Popescu 2006; Huang and Zheludev 2009). Previous researches have been proposed various methods to manage the outsidebands of superoscillation and acquire high quality images. In some cases (Rogers et al. 2012; Kosmeier et al. 2011), the contribution of the superoscillation outsidebands on the image quality can be suppressed by confocal microscopy imaging setup. In other approach, the outsidebands of superoscillation have been moved away from the subwavelength hotspot due to an appropriate window for imaging (Wong and Eleftheriades 2011, 2013). Studies also suggested that the outsidebands of superoscillation can remain with low energy for a weak subwavelength superoscillation hotspot (Rogers et al. 2013; Roy et al. 2014). As a result, several techniques have been introduced into two photons to suppress the superoscillation outsidebands in confocal scanning fluorescence microscopy (Dong et al. 2017). However, dealing with the superoscillation outsidebands remains a crucial consideration. Recently, the hybrid between the superoscillation and the subtraction method has been introduced to remove the outsidelobes of the superoscillation (Le et al. 2018). This approach requires two images in the imaging processing, which makes the method more time-consuming. In conclusion, there are always tradeoffs between resolution, viewing area, and time cost in the superoscillation imaging system.

Currently, binary optics technology has been widely used in achieving super-resolution (Dong et al. 2017; Le et al. 2018; Wang et al. 2012), producing non-diffraction beams (Wang et al. 2002, 2006; Wang and Gan 2001), generating longitudinally polarized light (Wang et al. 2008), and creating large-scale dark-spot optical traps for atoms (Wang and Gan 2001). Other applications of the binary phase mask are to generate multi point spread functions along the optical axis, which produces the applications of multi-planes (Yin et al. 2002). Therefore, the 3D imaging speed is improved. The binary phase mask can be used to obtain the anti-point spread functions, which can be used to cloak or hide the object (Wang et al. 2014). In addition, the binary phase mask can be used to design the superoscillation, which can generate a focus with a narrower central spot at the expense of increased energy in the sidelobes (Yin et al. 2002; Wang et al. 2014). The substantial sidelobes created by

the phase mask limited the resolution of the images. In order to suppress the sidelobes of superoscillation, a spatial filter in the detection path was introduced and the effect of sidelobes in the signal is eliminated by multiplying the PSF of the excitation beam and that of the detection beam. However, the zero-region of the superoscillation is still small, so intensity distribution of the sidelobes is still exited when the pinhole with the size of 0.5AU (Dong et al. 2017; Le et al. 2018; Kozawa et al. 2018). In this paper, we propose to use a binary phase mask with the radial polarization to obtain the superoscillation, which has big zero-region when achieving superoscillation in high numerical aperture, so the outsidelobes of the superoscillation can be suppressed effectively. In addition, the size of the pinhole is extended that leads to the improved effectiveness of light collected in the detection part.

2 Method

The focal effects of incident light propagating through an objective lens can be calculated by vector diffraction theory. The electric field near the focus plane can be obtained explicitly by the expression derived from the Debye integral (Richards and Wolf 1959),

$$\vec{E}\left(r_2, \varphi_2, z_2\right) = iC \iint_{\Omega} \sin(\theta) E_0 A(\theta, \varphi) P \times e^{i\Delta a(\theta,\varphi)} e^{ikn\left(z_2 \cos\theta + r_2 \sin\theta cons\left(\varphi-\varphi_2\right)\right)} d\theta d\varphi \tag{1}$$

where $\vec{E}\left(r_2, \varphi_2, z_2\right)$ is the electric field vector at the point (r_2, φ_2, z_2) expressed in cylindrical coordinates, C is the normalized constant, E_0 is the amplitude function of the input light, $A(\theta, \varphi)$ is a 3×3 matrix related to the structure of the imaging lens and P is Jones vector of the incident light. $\Delta a(\theta, \varphi)$ is the parameter of phase delay generated by the phase mask.

When the objective lens satisfies the sine condition, $A(\theta, \varphi)$ can be presented by,

$$A(\theta, \varphi) = \sqrt{\cos\theta} \begin{bmatrix} 1 + (\cos\theta - 1)\cos^2\varphi & (\cos\theta - 1)\cos\varphi\sin\varphi & -\sin\theta\cos\varphi \\ (\cos\theta - 1)\cos\varphi\sin\varphi & 1 + (\cos\theta - 1)\sin^2\varphi & -\sin\theta\sin\varphi \\ \sin\theta\cos\varphi & \sin\theta\sin\varphi & \cos\theta \end{bmatrix} \tag{2}$$

In the case of the incidence light with spatial non-uniform polarization, Jones vector of radial polarization is presented by,

$$\begin{pmatrix} p_x \\ p_y \\ p_z \end{pmatrix} = \begin{pmatrix} \sin\theta \\ \cos\theta \\ 0 \end{pmatrix} \tag{3}$$

In this paper, the high NA value which is used to perform the simulation is equal to 1.41 and the sample is placed in the medium whose refractive index is 1.518. In order to extend the zero-region of superoscillation, we use the binary phase mask with the radial polarization. In order to extend the zero-region of superoscillation, the binary phase mask will be optimized. The optimal conditions extend the zero-region of superoscillation are: (1) The zero-region of superoscillation is bigger than TH_1 value; (2) the full width half maximum (FWHM) of the central lobe of the superoscillation PSF is smaller than TH_2; (3) the radial number of the binary phase mask is the smallest. We propose the initial conditions such as $TH_1 = 1\lambda$ and $TH_2 = 0.259\lambda$. Based on the initial conditions above, we obtain

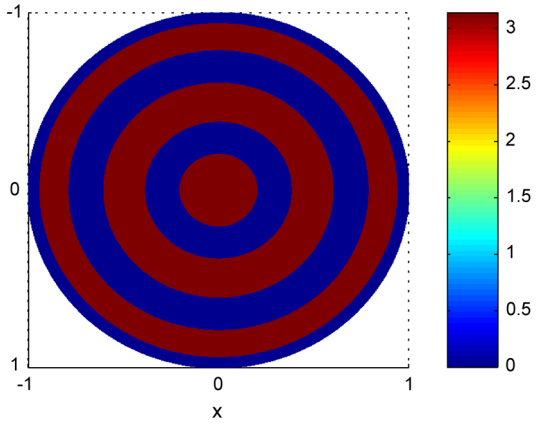

Fig. 1 The binary phase mask include radial values of $r_1 = 0.2$, $r_2 = 0.39$, $r_3 = 0.6$, $r_4 = 0.793$, $r_5 = 0.935$, $r_6 = 1$

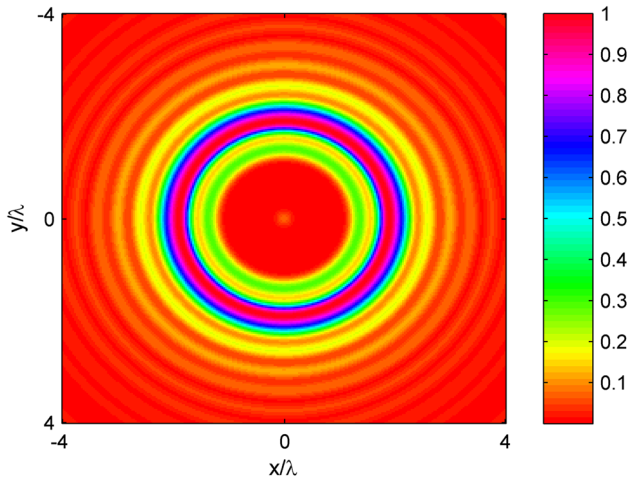

Fig. 2 The superoscillation PSF with the binary phase mask and radial polarization

the parameters of the binary phase mask as shown in Fig. 1. It is clear that the binary phase mask includes radial values of $r_1 = 0.2$, $r_2 = 0.39$, $r_3 = 0.6$, $r_4 = 0.793$, $r_5 = 0.935$ and $r_6 = 1$.

3 Simulation results

The superoscillation PSF is shown in Fig. 2. As Fig. 2 indicates, the superoscillation PSF can is divided into three parts: the insidelobes, the zero-region and the outsidelobes. The insidelobes of superoscillation is low intensity values, while the outsibelobes of superoscillation are high intensity values. The zero-region is used to divide between insidelobe and outsidelobes regions. In order to suppress the effect of the outsidelobes of superoscillation, we want to extend the radial of the zero-region of the superoscillation. In this paper, we can extend the radius of zero-region to 1λ for the high numerical aperture. For a big zero-region of the superoscillation, the outsidelobes of superoscillation can be reduced remarkably. The PSF of conventional confocal microscopy is shown

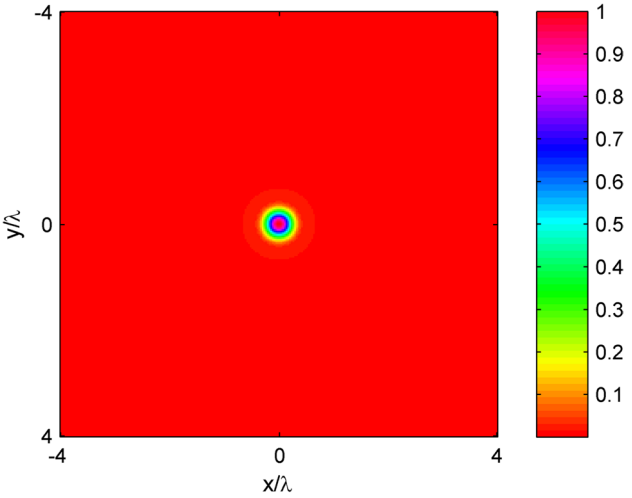

Fig. 3 The PSF of conventional confocal microscopy

in Fig. 3 as a comparison. As Figs. 2 and 3 show, the insidelobes of the superoscillation PSF is smaller than the PSF of conventional confocal microscopy. Here, the FWHM is used to measure the effectiveness of the imaging performance. In Fig. 3, the FWHM values of PSF of the superoscillation and conventional confocal microscopy are set to 0.259λ and 0.405λ, which means that the FWHM of superoscillation PSF is improved 1.56 times compared with the conventional confocal microscopy.

Next, we consider the performance of the proposed PSF in confocal fluorescence microscopy. In order to show the effectiveness of the proposed method reducing outsidelobes of superoscillation, we consider the overall system PSF. As shown in Ref. Le et al. (2018), the outsidelobes of the superoscillation PSF can be reduced by multiplying the PSFs of the excitation and detection beams. In addition, the PSF of the detection part is convolved with a small pinhole. The size of the pinhole is set to 0.6AU (1AU is equal to 1.22λ/NA). The size of the pinhole is larger in comparison with the previous papers (Dong et al. 2017; Le et al. 2018; Kozawa et al. 2018). The overall system PSF can be presented by,

$$\mathrm{h}_{overall} = [h_{Illu} \times (h_{\mathrm{dete}} \otimes \mathrm{pinhole})] \tag{4}$$

Based on the use of Eq. (4), the overall system PSFs of conventional confocal microscopy and the superoscillation are shown in Fig. 4. The overall system PSF of the superoscillation has a smaller width than that of conventional confocal microscopy, which means that the superoscillation PSF can be used to obtain high resolution. It is clear that the outsidelobes of the superoscillation are also removed, which means that when the big zero-region is generated and the effect of outsidelobes of superoscillation is effectively reduced. The profiles of the PSFs of conventional confocal microscopy and the superoscillation are plotted in Fig. 5. The FWHM of the superoscillation PSF is smaller than that of conventional confocal microscopy. In addition, it can be seen that the outsidelobes intensity of superoscillation is very low, which is only about 2% of the peak intensity value of the superoscillation PSF.

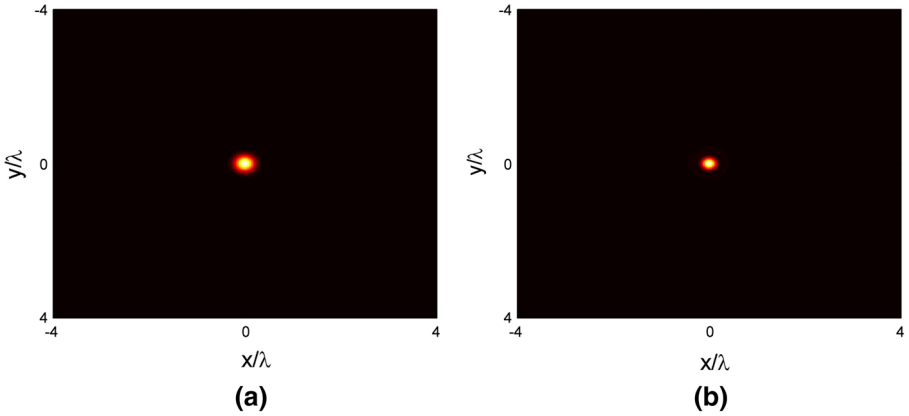

Fig. 4 The overall system PSFs of **a** conventional confocal microscopy and **b** the superoscillation

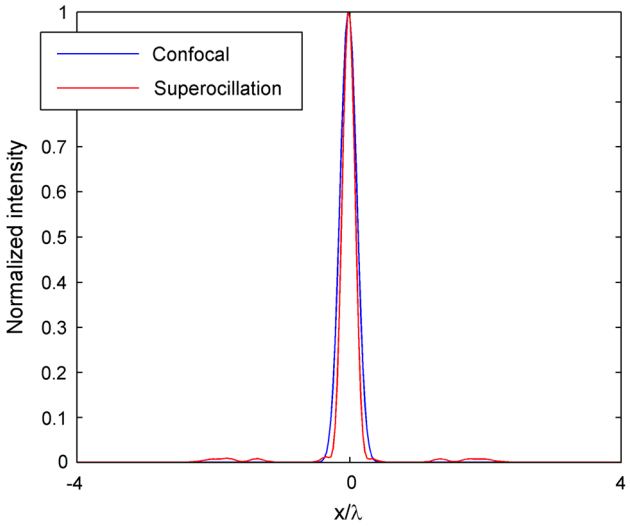

Fig. 5 The profiles of conventional confocal microscopy and the superoscillation PSFs

In order to highlight the effectiveness of the proposed method, we evaluate the actual imaging performance under a noisy background in the simulation. The recorded image, g, can be presented as,

$$g = o \otimes h_{overall} + n \tag{5}$$

where o is the object and n is the noise.

The starting image is shown in Fig. 6a. As Fig. 6a shows, the image includes two parts: the first part in the left of Fig. 6a and the second part in the right of Fig. 6a. The two parts include three points. However, the distance between the points in the first part is bigger than that in the second part. The distances between circles in the first and second grounds are 0.468λ and 0.281λ, respectively. Figure 6b and c depict the image of conventional confocal microscopy and the image of the superoscillation, respectively. As can be seen that

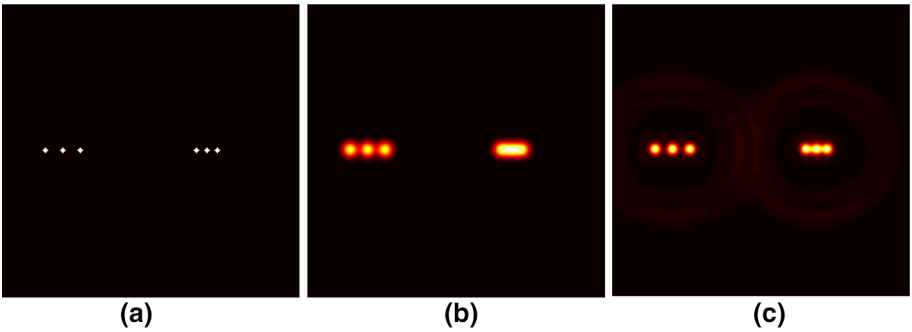

Fig. 6 Simulation images for conventional confocal microscopy and superoscillation, the size of images is $8\lambda \times 8\lambda$: **a** the original image, **b** the simulation of conventional confocal microscopy, and **c** the simulation of the proposed method. In the original image, the circles are divided into two groups: the first group includes three circles in the left and the second group includes three circles in the right

the resolution of superoscillation is better than that of conventional confocal microscopy. The points in the first part of the conventional confocal microscopy is discriminated, but fails to discriminate the points in the second part, while the superoscillation can discriminate the points in the both two parts. It is clear that the vague background, which is caused by the outsidelobes of superoscillation, is reduced remarkably. The profiles of images achieved by conventional confocal microscopy and the superoscillation, which are measured via the centers of circles, are indicated in Fig. 7. The intensity values at the central positions of the points of the superoscillation are similar and the background is very low. The peak intensity value of background is about 5% compared to the peak intensity of the points, which means that the proposed method can acquire high resolution and the background of the outsidelobes of the superoscillation is reduced remarkably.

Finally, we investigate the effect of noise in the proposed method. Here, the white Gaussian noise is added in simulation images of the superoscillation. Figure 8 shows the image of the superoscillation in Fig. 7 after adding the white Gaussian noise. Figure 8a, b and c show the results with the white Gaussian noise of 60SRN, 40SRN and 20SNR. As Fig. 8 shows, the noise results in the reduction of the quality of images. As the noise

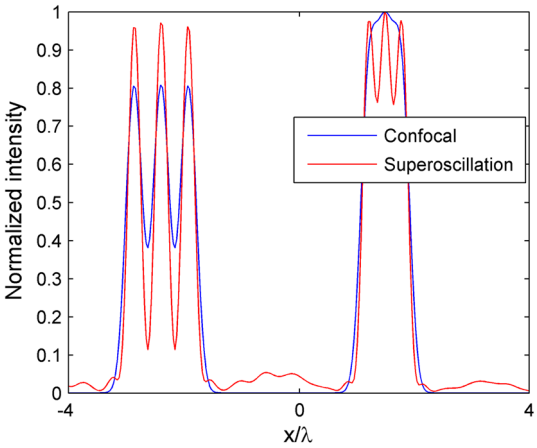

Fig. 7 Profiles of images obtained by the conventional confocal microscopy and the proposed method. The blue line is the profile of the image obtained by conventional confocal microscopy and the red line is that of the proposed method. (Color figure online)

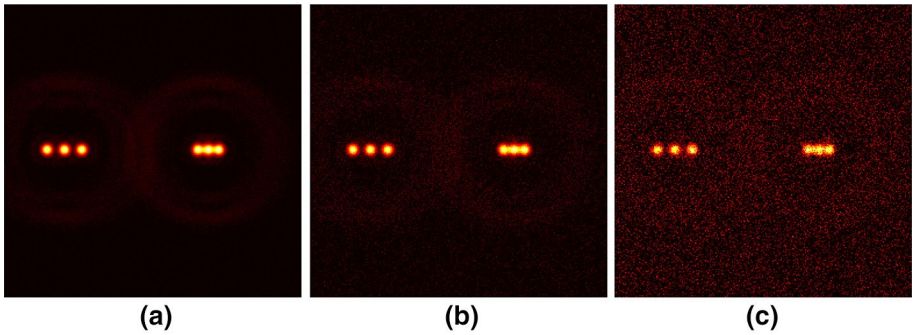

Fig. 8 The simulation images for different noise levels. The noise values for Figs. **a**, **b** and **c** are set to 60SNR, 40SNR and 20SNR, respectively. The size of the image is 8λ × 8λ

density of white Gaussian noise increases, the effect of noise on image quality also increases. As Fig. 8c shows, when the white Gaussian noise is 20SNR, the discrimination of the points in the second part is significantly reduced.

In order to improve the imaging performance of the proposed method, an amplitude mask is added, while the phase mask does not still change as shown in Fig. 1. Here, we use an amplitude mask, P(r) = r^2, as shown in Fig. 9a. When the amplitude mask is inserted, the superoscillation PSF is shown in Fig. 9b showing the intensity value of the insidelobe increases in comparison to the peak intensity value of the outsibelobes. Figure 9c presents the image of superoscillation when the amplitude mask is added. It can be seen that the background of the outside lobes of superoscillation is strongly suppressed.

4 Conclusion

In this paper, we have proposed a method extending the zero-region of the superoscillation to obtain high resolution and to suppress the background of the outsidelobes of the superoscillation PSF. A binary phase mask with radial polarization generating the superoscillation PSF is introduced and a big zero-region of the superoscillation PSF is obtained. The simulation results are based on the evaluation approaches of PSF and demonstrated the proposed method's effectiveness. The effectiveness of the proposed method can be

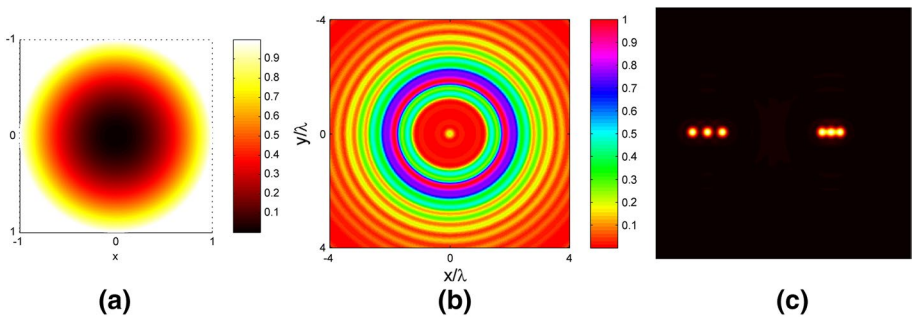

Fig. 9 **a** Amplitude mask, **b** the point spread function, **c** simulation image, the size of the image is 8λ × 8λ

improved further by adding more suitable amplitude masks. In the future, the experimental results will be acquired.

Acknowledgements This work was supported by Vietnam National Foundation for Science and Technology Development (NAFOSTED) under Grant number (103.03-2018.08).

References

Aharonov, Y., Vaidman, L.: Properties of a quantum system during the time interval between two measurement. Phys. Rev. A **41**(1), 11–20 (1990)

Aharonov, Y., Albert, D.Z., Vaidman, L.: How the result of a measurement of a component of spin-1/2 particle can turn out to be 100. Phys. Rev. Lett. **60**, 1351–1354 (1998)

Berry, M.V., Popescu, S.: Evolution of quantum superoscillations and optical superresolution without evanescent waves. J. Phys. A. **39**, 6965 (2006)

Betzig, E., Patterson, G.H., Sougart, R., et al.: Imaging intracellular fluorescent proteins at nanometer resolution. Science **313**, 1642–1645 (2006)

Classen, A., Zanthier, J.V., Scully, M.O., Agarwal, G.S.: Superresolution via structured illumination quantum correlation microscopy. Optica **4**(6), 480 (2017)

Dong, X.H., Wong, A.M.H., Kim, M., Eleftheriades, G.V.: Superresolution far-field imaging of complex objects using reduced superoscillating ripples. Optica **4**(9), 1126–1133 (2017)

Ferreira, P.J.S.G., Kempf, A.: Superoscillations: faster than Nyquist rate. IEEE Trans. Signal Process. **54**, 3732–3740 (2006)

Gao, P., Prunsche, B., Zhou, L., Nienhaus, K., Nienhaus, G.U.: Background suppression in fluorescence nanoscopy with stimulated emission double depletion. Nat. Photon. **11**, 163–169 (2017)

Gustafsson, M.G.L.: Nonlinear structured-illumination microscopy: wide-field fluorescence imaging with theoretically unlimited resolution. PNAS **102**(37), 13081–13086 (2005)

Hell, S.W., Wichmann, J.: Breaking the diffraction resolution limit by stimulated emission: stimulated-emission-depletion fluorescence microscopy. Opt. Lett. **19**, 780–782 (1994)

Hess, S.T., Giriajan, Y.P.K., Mason, M.D.: Ultra-high resolution imaging by fluorescence photoactivation localization microscopy. Biophys. J. **91**(11), 4258–4272 (2006)

Huang, F.M., Zheludev, N.I.: Super-resolution without evanescent waves. Nano Lett. **9**, 1249–1254 (2009)

Huang, B., Wang, W., Bates, M., Zhuang, X.: Three-dimensional super-resolution imaging by stochastic optical reconstruction microscopy. Science **319**, 810–813 (2008)

Korobcheyvskaya, K., Peres, C., Li, Z., Antipov, A., Sheppard, C.J.R., Diaspro, A., Bianchini, P.: Intensity weighted subtraction microscopy approach for image contrast and resolution enhancement. Sci. Rep. **6**, 25816 (2016)

Kosmeier, S., Mazilu, M., Baumgartl, J., Dholakia, K.: Enhanced two-point resolution using optical eigenmode optimized pupil functions. J. Opt. **13**, 105707 (2011)

Kozawa, Y., Matsunaga, D., Sato, S.: Superresolution imaging via superoscillation focusing of a radially polarized beam. Optica **5**(2), 86–92 (2018)

Kuang, C., Li, S., Liu, W., Hao, X., Gu, Z., Wang, Y., Ge, J., Li, H., Liu, X.: Breaking the diffraction barrier using fluorescence emission difference miscroscopy. Sci. Rep. **3**, 1441–1446 (2013)

Le, V., Kuang, C., Liu, X.: Extended depth-of field imaging by both radially symmetrical conjugating phase masks with spatial frequency post-processing. Opt. Commun. **411**, 80–87 (2018a)

Le, V., Wang, X., Kuang, C., Liu, X.: Background suppression in confocal scanning fluorescence microscopy with superoscillations. Opt. Commun. **426**, 541–546 (2018b)

Le, V., Wang, X., Kuang, C., Liu, X.: Resolution enhancement of confocal scanning microscopy using low-intensity imaging part of point spread function. Opt. Eng. **57**(5), 053106-1 (2018c)

Richards, B., Wolf, E.: Electromagnetic diffraction in optical systems. 2. Structure of the image field in an aplanatic system. Proc. R. Soc. A **253**, 358–379 (1959)

Rogers, E.T.F., Lindberg, J., Roy, T., Savo, S., Chad, J.E., Dennis, M.R., Zheludev, N.I.: A super-oscillatory lens optical microscope for subwavelength imaging. Nat. Mater. **11**, 432–435 (2012)

Rogers, E.T.F., Savo, S., Lindberg, J., Roy, T., Dennis, M.R., Zheludev, N.I.: Super-oscillatory optical needle. Appl. Phys. Lett. **102**, 031108 (2013)

Roy, T., Rogers, E.T.F., Yuan, G., Zheludev, N.I.: Point spread function of the optical needle super-oscillatory lens. Appl. Phys. Lett. **104**, 231109 (2014)

Rust, M.J., Bates, M., Zhuang, X.: Sub-diffraction-limit imaging by stochastic optical reconstruction microscopy (STORM). Nat. Methods **3**, 793–796 (2006)
Segawa, S., Kozawa, Y., Sato, S.: Resolution enhancement of confocal microscopy by subtraction method with vector beams. Opt. Lett. **39**(11), 3118–3121 (2014)
Wan, C., et al.: Three-dimensional visible-light capsule enclosing perfect supersized darkness via antiresolution. Laser Photon. Rev. **5**, 743–749 (2014)
Wang, H.F., Gan, F.X.: High focal depth with pure phase apodizer. Appl. Opt. **40**, 5658–5662 (2001)
Wang, H.F., Chen, Z.Y., Gan, F.X.: Phase-shifting apodizers for increasing focal depth. Appl. Opt. **41**, 5263–5266 (2002)
Wang, H.F., Shi, L.P., Yuan, G.Q., Miao, X.S., Tan, W.L., Chong, T.C.: Subwavelength and super-resolution nondiffraction beam. Appl. Phys. Lett. **89**, 171102 (2006)
Wang, H.F., Shi, L., Lukyanchuk, B., Sheppard, C.J.R., Chong, T.C.: Creation of a needle of longitudinal polarized light in vacuum using binary optics. Nat. Photon. **2**, 501–505 (2008)
Wang, H.F., Sheppard, C.J.R., Koustuban, R., Ho, S.T., Vienne, G.: Fighting against diffraction: apodizer and near field diffraction structures. Laser Photon. Rev. **6**, 354–392 (2012)
Wang, H., et al.: Creation of an anti-imaging system using binary optics. Sci. Rep. **6**, 33064 (2014)
Wong, M.H., Eleftheriades, G.V.: Temporal pulse compression beyond the Fourier transform limit. IEEE Trans. Microw. Theory Tech. **59**, 2173–2179 (2011)
Wong, M.H., Eleftheriades, G.V.: An optical super-microscope for far-field, real-time imaging beyond the diffraction limit. Sci. Rep. **3**, 1715 (2013)
Yin, J.P., Gao, W.J., Wang, H.F., Long, Q., Wang, Y.Z.: Generation of dark hollow beams and the applications in laser cooling of atoms and all optical-type Bose-Einstein condensation. Chin. Phys. B **11**, 1157 (2002)